Inter-turn Short Circuit Fault Diagnosis and Severity Estimation for Wind Turbine Generators

Inter-turn Short Circuit Fault Diagnosis and Severity Estimation for Wind Turbine Generators

Jingyi Yan[1,2], Soroush Senemmar[1,3], and Jie Zhang[1,2,3]

[1]Center for Wind Energy, The University of Texas at Dallas, Richardson, TX 75080, USA
[2]Department of Mechanical Engineering, The University of Texas at Dallas, Richardson, TX 75080, USA
[3]Department of Electrical and Computer Engineering, The University of Texas at Dallas, Richardson, TX 75080, USA

E-mail: {jingyi.yan, soroush.senemmar, jiezhang}@utdallas.edu

Abstract. While preventive maintenance is crucial in wind turbine operation, conventional condition monitoring systems face limitations in terms of cost and complexity when compared to innovative signal processing techniques and artificial intelligence. In this paper, a cascading deep learning framework is proposed for the monitoring of generator winding conditions, specifically to promptly detect and identify inter-turn short circuit faults and estimate their severity in real time. This framework encompasses the processing of high-resolution current signal samples, coupled with the extraction of current signal features in both time and frequency domains, achieved through discrete wavelet transform. By leveraging long short-term memory recurrent neural networks, our aim is to establish a cost-efficient and reliable condition monitoring system for wind turbine generators. Numeral experiments show an over 97% accuracy for fault diagnosis and severity estimation. More specifically, with the intrinsic feature provided by wavelet transform, the faults can be 100% identified by the diagnosis model.

1. Introduction

Effective condition monitoring of wind turbines (WTs) is one of the most important tasks to ensure their reliable operation, energy production optimization, and minimization of maintenance expenses [1–4]. Traditional methods like direct sensing or periodic inspections, while valuable, confront limitations in cost and efficacy. Recent advancements in signal processing and artificial intelligence (AI) offer exciting possibilities for comprehensive fault detection across all stages of WT systems.

1.1. Literature Review

A comprehensive WT system comprises several mechanical and electrical subsystems, each playing a crucial role in the power conversion process. The workflow typically involves a rotor hub, rotor blades, and a yaw system to harness kinetic energy from the wind. This energy is then transmitted through a low-speed shaft, gearbox, and high-speed shaft, converting kinetic power to mechanical power, speeding up rotation, and reducing torque [2; 5]. The mechanical system, illustrated in Fig. 1, encompasses these subsystems. As a key component in both mechanical and electrical systems, the generator converts mechanical power to electrical power. The electrical system further includes a power converter and transformer to step up voltage

before integrating into the electrical network. Auxiliary subsystems include a tower providing support for the overall electrical and mechanical systems, a nacelle housing internal equipment atop the tower and behind the yaw, a brake for rotor maintenance or curtailment occasions, and a Supervisory Control and Data Acquisition (SCADA) system for data collection and wind turbine control [2].

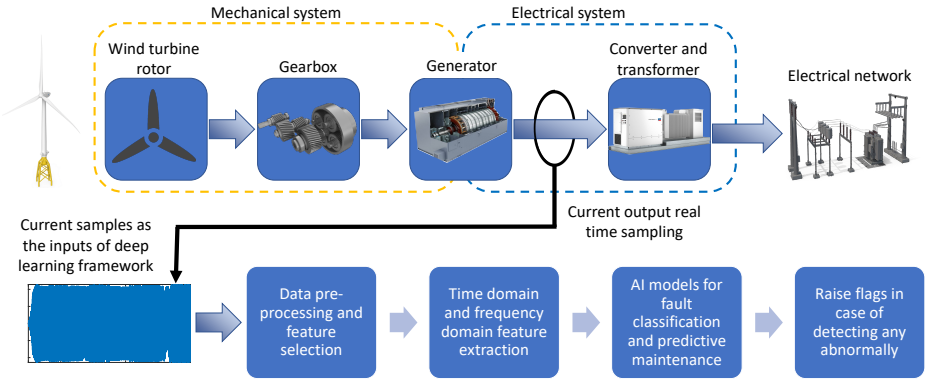

Figure 1: Overall framework of the proposed machine learning-enabled condition monitoring

Dao et al. [6] have conducted a comprehensive analysis covering more than 18,500 WTs and approximately 93,000 operating years onshore and offshore across Europe, Asia, and America. The findings indicate that generators and gearboxes emerge as the most critical subsystems, both onshore and offshore, in terms of downtime. The report further reveals that generators rank second for the longest onshore downtime and offshore repair time per failure. Unfortunately, onshore repair time and offshore downtime data were not collected in the report. Consequently, effective condition monitoring of generators in wind turbines becomes imperative to mitigate downtime, reduce operation and maintenance (O&M) costs, and accordingly enhance overall profitability.

Addressing this need, Jin et al. [7] leverage SCADA data for detecting and identifying abnormalities in WT generators. The methodology involves constructing a healthy model in Mahalanobis space (MS) during the training stage. In the online monitoring stage, the Mahalanobis distance (MD) of new SCADA signals is calculated, and an abnormality alarm is triggered if it surpasses a threshold value determined through Johnson transformation and inversion of the healthy system. Abnormalities are then isolated through distribution and correlation analysis of signal features. The effectiveness of this approach is validated through two case studies, affirming its efficacy in wind turbine generator fault prognosis and identification.

Attallah et al. [8] identify 11 WT generator operating conditions at no load, including a healthy mode, a stuck rotor fault, a cooling fan failure, and 8 inter-turn short circuit faults (ITSCFs) characterized by varying short-circuit percentages and faulty phases in the stator winding. Leveraging thermal infrared (IR) images, the classification accuracy experiences improvement through progressive enhancements in the classifier methodology. Initially employing a single convolutional neural network (CNN), the classifier's accuracy is further elevated by combining results from three CNNs with discrete wavelet transform (DWT) before classification, and introducing principle component analysis (PCA) between DWF and the classifier.

1.2. Research Objectives

This paper introduces a cascading deep learning framework, grounded in signal processing, designed for the diagnosis of ITSCFs and the estimation of severity in the context of wind turbine Double-Fed Induction Generator (DFIG) systems. Such framework is built on top of our prior studies on complex systems monitoring and fault detection [9–12]. Initially, 16 operating modes

of WT DFIG are identified and simulated using MATLAB. Each stator winding short-circuit scenario, in addition to a healthy mode, includes five instances with decreasing short circuit resistance, totaling to 16 scenarios to mimic winding insulation degradation ($1 + 3 \times 5 = 16$). High-resolution and high-frequency three-phase generator current signals are recorded, and deep features are extracted through DWT. The cascading approach employs similar Long Short-Term Memory (LSTM) Recurrent Neural Networks (RNNs) for fault detection and severity estimation, thereby enhancing the overall diagnostic capability.

Figure 1 provides an overview of our proposed approach. The primary objective is to continuously monitor the generator stator winding in the WT system for promptly identifying any anomalies in real time. The key contributions of this paper are summarized as follows:

- The effective definition and simulation of multiple inter-turn insulation degradation scenarios using MATLAB/Simulink.
- The detection and identification of ITSCFs with high accuracy and robustness using the proposed cascading deep learning framework.
- Real-time estimation of insulation degradation severity to ensure reliable WT operation and optimize energy production.

The rest of the paper is organized as follows. The problem formulation and simulation are described in Section 2. The proposed condition monitoring system with a cascading framework is introduced in Section 3. Section 4 presents the numerical experiments and their results, followed by conclusion and future work in Section 5.

2. Problem Formulation

The degradation of winding insulation is the primary trigger for ITSCFs. While incipient ITSCF remain undetected, it can develop into more severe phase-to-phase and phase-to-ground faults [13]. In this section, a WT example in MATLAB\Simulink is leveraged to simulate ITSCF under various scenarios of winding insulation degradation.

2.1. Wind Turbine System

For our investigation, we utilize a 1.5 MW MATLAB/Simulink WT example sourced from The MathWorks, Inc. [14]. This example encompasses both mechanical and electrical domains, providing a comprehensive framework to delineate various operating scenarios. The model comprises rotor blades in 35.25 m radius, a gearbox model featuring a one-stage planetary and two-stage helical gear arrangement, a lumped star-connected DFIG subsystem, a 1.8 MW transformer model, and a grid model. The default wind profile is leveraged in this research, and the wind speed V is defined by Eq. (1), where t is the simulated time in second, and wind speed in m/s.

$$\mathrm{V} = \begin{cases} 15 & t < 45 \\ t - 30 & 45 \leq t < 52 \\ 22 & t \leq 80 \end{cases} \tag{1}$$

In the WT model, four operating modes, i.e. startup, generating, pitch brake, and park brake modes, are determined based on prevailing wind and turbine speed conditions by the controller module. Rather than the steady working condition, the simulation includes all four modes to capture the generator's variant conditions while implemented in WT. The detailed information about the modeling, operating states, and power generation can be found in [14].

2.2. Inter-turn Short Circuit Fault (ITSCF) Scenarios

The stator winding of the generator is modeled based on the equivalent impedance of the generator. The ITSCF is simulated through dividing a healthy winding (0.0027 Ω) into both healthy (80%) and faulty (20%) segments. A short-circuit bypath is incorporated into the faulty winding. ITSCF severity is ranked on the faulty winding ratio, from 0% (healthy condition) to 40% in [15], and to 62.5% in [16]. In this paper, however, we consider the nature of insulation material degradation, and define the short circuit resistance as the degradation indicator. Similar research can be found in [17; 18]. While healthy winding means such bypath has infinite resistance, a series of decreasing resistance $R_s \in \{1, 0.1, 0.01, 0.001, 0.0001\}(\Omega)$ simulate the insulation degr / and faulty win ı from normal o t phases.

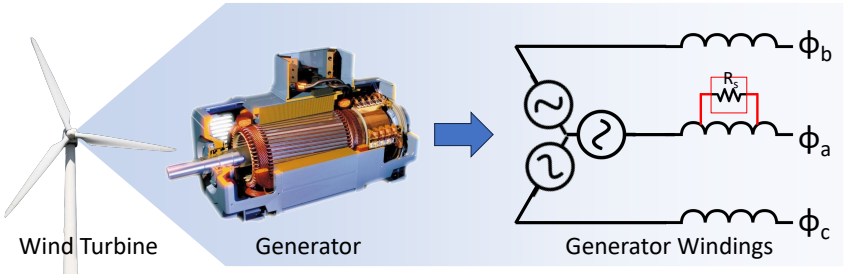

Figure 2: ITSCF condition in the stator of a WT generator

From a simulation point of view, the stator winding insulation degradation can be modeled by an ITSCF inside the stator. Even though the powerful simulation model can provide us infinite dataset, the real-world unbalanced healthy and faulty operating data structure available to train the condition monitoring model is considered at this stage. To achieve so, the faulty operation duration is kept short in a cycle, mimicking the sparse dataset we can obtain from wind farm to train the condition monitoring model, which doesn't mean that we analyze the short duration short circuit situation. Therefore, all faults are intentionally triggered between 29.5 and 30 seconds within an 80-second simulation in the case study. Such time information will not input into the condition monitoring system.

Figure 3 shows the generator phase A current with different ITSCFs happen at 29.5-30 seconds in a cycle of WT operation. The generator is enabled to generate power only in generating and pitch brake modes. The pitch brakes due to the turbine rotor speed is higher than the limited speed and the generated current soaring abnormally, that prevents mechanical and electrical failure. The current variance according to the variant kinetic power obtained by the rotor is kept while analysing the ITSCF characteristic of the induction generator in WT. Five different short circuit resistors simulate the severeness of the short circuit, i.e., the stator winding insulation degradation level. When the insulation degradation is severe, the short circuit resistor is lower and consequently the current has a bigger jump, as illustrated in Fig. 3. Fig. 3 further shows that as the winding insulation degradation intensifies, indicated by lower short circuit resistance, the faulty phase current exhibits a corresponding increase.

Figure 4 shows the impact of ITSCF on the three-phase currents in the generator. The differentiation of three-phase current under short circuit resistance $R = 0.0001\Omega$ situation illustrates the asymmetric phase current phenomena caused by ITSCFs. And the zoom-in box in Fig. 4 (b) again presents the three-phase current jump in ITCSF condition. The condition monitoring system's diagnosis model will not only tell us if the WT generator is normally operating or not, but also classify which phase is at fault. While the current rises are notably discernible compared to normal operation under similar conditions, distinguishing these

variations becomes challenging when compared to other operational scenarios. Since even in the severest situation of the case study, the short current is still lower than the maximum current in the pitch brake mode. And therefore, the proposed deep learning framework is developed to distinguish whether the current soaring up is due to the short circuit fault or other operating conditions, like under the high wind speed environment.

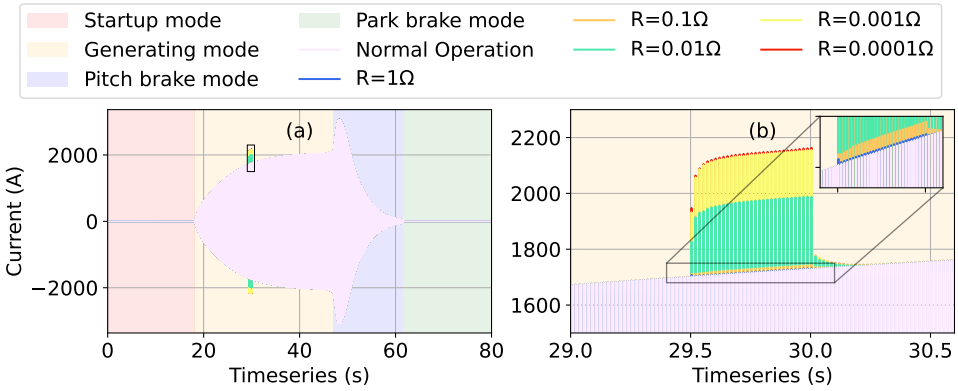

Figure 3: (a) Phase A current comparison on different phase A winding short circuit resistance; (b) zoom-in figure of (a)

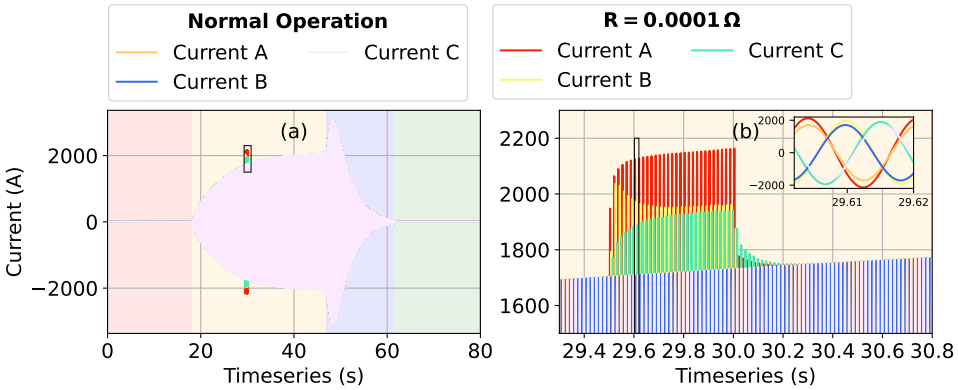

Figure 4: (a) Three-phase current comparison on healthy condition and phase A ITSCF condition; (b) zoom-in figure of (a)

3. Cascading Condition Monitoring Framework

Figure 5 illustrates the proposed cascading condition monitoring framework, consisted of four main components: data sampling, signal analysis, fault diagnosis, and severity estimation. Following the recording of three-phase current signals, we employ a DWT to extract both time and frequency domain features. Simultaneously, a fault diagnosis model is deployed to detect and isolate ITSCFs. Furthermore, for each winding in every phase, three distinct severity estimation models are meticulously trained.

3.1. Signal Analysis

Both the Short-Term Fourier Transform (STFT) and wavelet transform are prominent signal processing techniques for extracting frequency features from time series data, with the objective of preserving crucial time domain information. Notably, the wavelet transform is esteemed for its superior time-frequency localization capability, as acknowledged in the literature [19].

In contrast to sine waves characterized by infinite energy, a wavelet concentrates energy at a point and oscillates out rapidly. For any signal function $f(n)$ residing in the Hilbert space $L^2(\mathbb{R})$, it can be dissected through the linear combination of two series. The first series

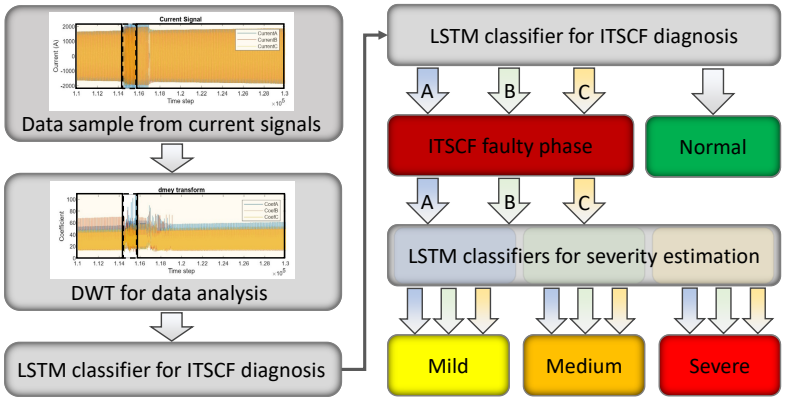

Figure 5: The overall framework of cascading condition monitoring

comprises orthonormal wavelet functions denoted as $\psi \in L^2(\mathbb{R})$, while the second series involves orthonormal scaling functions represented by $\phi \in L^2(\mathbb{R})$, as illustrated in Eq. (2).

$$f(n) = \sum_{k\in\mathbb{Z}} a_{j_0,k}\phi_{j_0,k}(n) + \sum_{\substack{j\in\mathbb{Z}\\ j\geq j_0}} \sum_{k} d_{j,k}\psi_{j,k}(n) \tag{2}$$

where j_0 is the level of decomposition. $a_{j_0,k}$ and $d_{j,k}$ are approximation and detail coefficients. Due to the orthonormal characteristic of wavelet and scaling functions, they can be derived through the inner product of the signal function $f(n)$ and their respective bases:

$$a_{j_0,k} = \langle f(n), \phi_{j_0,k}(n)\rangle \tag{3}$$

$$d_{j,k} = \langle f(n), \psi_{j,k}(n)\rangle \tag{4}$$

Consequently, the time and frequency features are extracted by those coefficients, with carefully selected wavelet and scale functions. The decomposition in Eq. (2) effectively captures the high frequency through the wavelet function and keeps the time resolution through the scaling function.

3.2. Long Short-Term Memory Networks

Operating as a dynamic neural network, RNNs have the capability to capture both spatial and temporal patterns from input data through a feedback mechanism within the neuron structure [20]. In contrast, Long Short-Term Memory (LSTM) networks specifically address the gradient vanishing problem inherent in traditional gradient-based RNNs. To mitigate this issue, the LSTM model introduces two additional gates – the forget gate and the output gate. The mathematical formulations of the LSTM structure are described as follows.

$$f_t = \sigma(W_f \cdot [h_{t-1}, x_t] + b_f) \tag{5}$$

$$i_t = \sigma(W_i \cdot [h_{t-1}, x_t] + b_i) \tag{6}$$

$$O_t = \sigma(W_o \cdot [h_{t-1}, x_t] + b_o) \tag{7}$$

where x_t is the input vector, h_{t-1} is the output of the previous block, f_t, i_t, and O_t represent the forget gate, input gate, and output gate at timestamp t, respectively. The W, b pair functions as the weight and bias parameters for each gate, while σ assumes the role of the "sigmoid" function. Equation (5) determines whether to retain or discard the vector for this cell, encapsulating the decision-making process. Simultaneously, Eq. (6) represents the new input vector. Lastly, the output gate in Eq. (7) contributes to the activation of the cell's output.

$$\tilde{C}_t = tanh(W_c \cdot [h_{t-1}, x_t] + b_c) \tag{8}$$

$$C_t = f_t \times C_{t-1} + i_t \times \tilde{C}_t \tag{9}$$

where $\tilde{C}_t$ is the output candidate of the cell, C_t and C_{t-1} are the memory from the current and previous cell, respectively.

$$h_t = O_t \times tanh(C_t) \tag{10}$$

where h_t is the output of the current cell at timestamp t.

4. Experimental Results

After collecting current signals from 15 different faulty scenario simulations, only each 0.5-second faulty condition period is captured as faulty condition. The transient state of the current, which can be observed at the beginning of the short circuit situation, is maintained in the case study. This is because in real cases, the short circuit can happen in a sudden resulting from the manufacturing defect like void in the insulation material. This incipient period is kept to guarantee the quick response capability of the condition monitoring system. Such transient state gradually diminishes and the steady state remains, together with the generator' response, which fluctuates in accordance with the turbine rotor speed, exhibiting both transient and steady state behaviors. The relative steady state with respect to short circuit current can also reflect the situation when the insulation degradation is slowly propagated. A whole 80-second simulation under normal operation is obtained for healthy dataset.

Based on the electrical characteristics depicted in Fig. 3, we establish three severity ranks for ITSCFs:

- **Mild Class:** A notification is triggered when $R_s \geq 0.1\,\Omega$.
- **Medium Class:** A flag is raised when $0.1\,\Omega > R_s > 0.001\,\Omega$.
- **Severe Class:** The WT should be shut down immediately when $R_s \leq 0.001\,\Omega$.

4.1. Computational Setup and Hyper-parameters

The experimental results are obtained from a computer equipped with an AMD Ryzen Threadripper Pro 5995WX featuring 64 cores and 128 CPUs, complemented by 512 GiB of RAM. All simulations and feature extraction processes are carried out using MATLAB version 2022a, while the implementation of deep learning models utilizes TensorFlow in version 2.15.0.

The Discrete Meyer wavelet function is employed for the implementation of the DWT in data processing. All deep learning models are designed with four layers and trained using the Adam optimizer and categorical cross-entropy loss function. Following iterative experimentation, the fault diagnosis model is configured with layers having 24, 48, 48, and 24 units, respectively. In contrast, the severity estimation models have layers with 24, 48, 24, and 12 units, respectively. To mitigate overfitting, 1/10 of the units in each layer are randomly dropped out during the training period. The fault diagnosis model undergoes 15 epochs with a batch size of 256, while the three severity estimation models undergo 30 epochs with a batch size of 512 each.

The input features of both diagnosis and prognosis models are the same: three phase current data and the first level approximation coefficient of each phase current after DWT, totally 6 input parameters. Every input includes preceding 50 time step signals for the LSTM model.

The division of training and testing sets is performed randomly in an 80:20 ratio. For diagnosis model, the training data for different classification, i.e. healthy, phase A fault, phase B fault, and phase C fault, are highly unbalanced. The ratio of healthy and single-phase fault period is $80/(0.5 * 5) = 32$ in the case study. Therefore, the dataset in faulty situation is randomly resampled in all classes to eventually have the same number of data points under different classes to train the model. A similar resampling process is implemented to the training set for prognosis models, but not for the testing set.

4.2. Results and Discussion

Both the fault diagnosis and severity estimation problems are treated as classification tasks. Since the naturally imbalanced data is maintained during the testing period, to ensure the evaluation of performance in underrepresented scenarios, such as the faulty condition in fault diagnosis and the medium severity condition in severity estimation, the averaged metrics are leveraged, which average the performance with respect to each detecting class as the overall metric value of the classifier. Four key metrics are evaluated in this study: averaged accuracy, averaged precision, averaged recall, and averaged F-measure. The calculation of these metrics can be found in [21].

To verified the necessity of DWT, comparative experiments with and without DWT coefficient input into the diagnosis model are conducted. The confusion matrices depicting fault diagnosis and insulation degradation severity estimation for the proposed method are illustrated in Fig. 6 and Fig. 7, where the number of samples in each class is scaled to 100 for the illustration purpose. Table 1 provides an overview of the evaluation metrics derived from these confusion matrices. A metric value closer to 100% indicates superior classification performance of the model. The comparison of diagnosis model with and without DWT input shows that the final gap between high accuracy of fault diagnosis and perfect can be bridged with the frequency information extracted by wavelet transform. The proposed method exhibits exceptional capability in ITSCF severity estimation, with all metric values surpassing 97%. While the overall accuracy for severity estimation is 97.39%, the proposed framework achieves an accuracy of 97.39%, as detailed in Table 1.

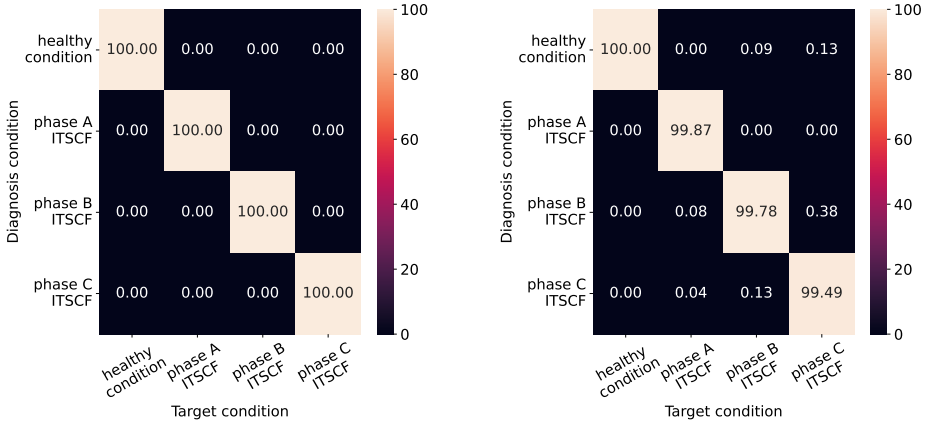

(a) Fault diagnosis with DWT (b) Fault diagnosis without DWT

Figure 6: Confusion matrices of fault diagnosis with and without DWT

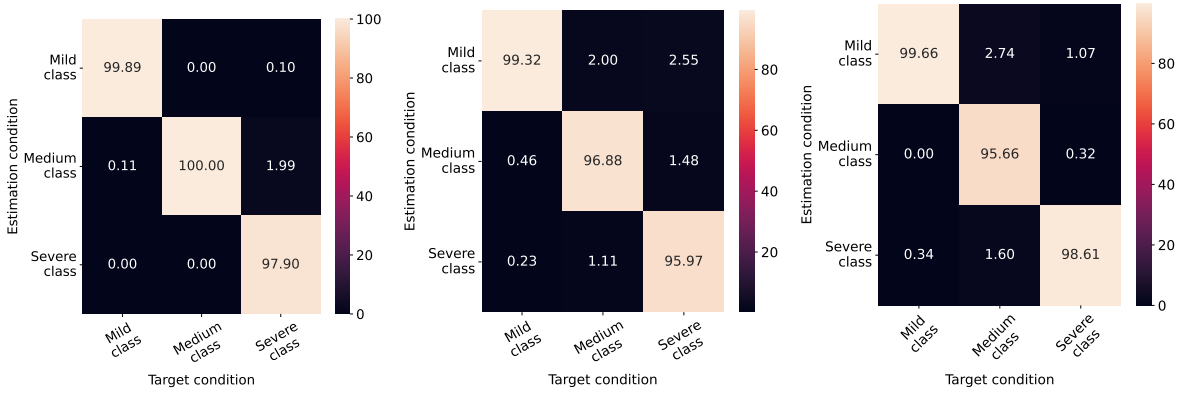

(a) Phase A severity estimation (b) Phase B severity estimation (c) Phase C severity estimation

Figure 7: Confusion matrices of severity estimation

Table 1: Evaluation metrics (%) for fault diagnosis and severity estimation performance

Model	Accuracy	Precision	Sensitivity	F1-score
Fault diagnosis with wavelet transform	100	100	100	100
Fault diagnosis without wavelet transform	99.79	99.83	99.79	99.81
Phase A severity estimation	99.26	98.51	99.26	98.87
Phase B severity estimation	97.39	97.20	97.39	97.28
Phase C severity estimation	97.98	98.60	97.98	98.27
Overall performance	97.39	97.20	97.39	97.28

It is essential to highlight that the fault diagnosis model not only detects anomalies but also identifies the specific phase where the anomaly occurs, encompassing various severity situations. The discernment of current variations under diverse operating conditions and ITSCF is achieved through the feature extraction facilitated by DWT and the implementation of LSTM.

5. Conclusion

In this paper, a novel, cost-effective, and highly reliable condition monitoring system for WT generator is proposed. This system uniquely harnesses high-resolution current signals directly sourced from the WT's operations. Initially, these real-time signals undergo a DWT, extracting intricate time and frequency features. This approach excels at pinpointing distinctive signatures within the signals, thus enabling the identification of a wide spectrum of potential issues encompassing malfunctions, abnormalities, and defects. Subsequently, four LSTM models are deployed to interpret these extracted features, spearheading the essential tasks of fault diagnosis, predictive maintenance, and reliable operation. These models possess exceptional capabilities not only for identifying ITSCFs but also for severity estimation. The development and training of the proposed deep learning framework rely on physics-based simulations. As the system refines its predictions against known outcomes, it sharpens its diagnostic abilities, distinguishing between normal and faulty states while extrapolating potential future deviations.

Potential future work will explore (i) more faulty scenarios in generators such as different faulty winding percentages and the faulty propagation to phase-to-phase and phase-to-ground faults, (ii) remaining life estimation on WT generator, and (iii) the application of this condition monitoring methodology to transformers.

Acknowledgments

This material is based upon work supported by the National Science Foundation under Grant Number 1916776 (Phase II IUCRC at UT Dallas: Center for Wind Energy Science, Technology and Research (WindSTAR)) and the WindSTAR I/UCRC Members. Any opinions, findings, and conclusions or recommendations expressed in this material are those of the author(s) and do not necessarily reflect the views of the National Science Foundation or WindSTAR members. The presenting author is grateful to the Center for Wind Energy at UT Dallas for providing support for conference registration and travel.

References

[1] Pulikollu R, Erdman W, Mclaughlin J, Alewine K, Sheng S, Bezner J. Wind Turbine Generator Reliability Analysis to Reduce Operations and Maintenance (O&M) Costs 2023;.

[2] Badihi H, Zhang Y, Jiang B, Pillay P, Rakheja S. A comprehensive review on signal-based and model-based condition monitoring of wind turbines: fault diagnosis and lifetime prognosis 2022. *Proceedings of the IEEE*;**110**:754-806.

[3] Li B, Sedzro K, Fang X, Hodge BM, Zhang J. A clustering-based scenario generation framework for power market simulation with wind integration 2020. *Journal of Renewable and Sustainable Energy*;**12**:036301.

[4] Li H, Rahman J, Zhang J. Optimal planning of co-located wind energy and hydrogen plants: a techno-economic analysis 2022. *J Phys: Conf Series*;**2265**.

[5] Qiao W, Lu D. A survey on wind turbine condition monitoring and fault diagnosis—part I: components and subsystems 2015. *IEEE Transactions on Industrial Electronics*;**62**:6536-45.

[6] Dao C, Kazemtabrizi B, Crabtree C. Wind turbine reliability data review and impacts on levelised cost of energy 2019. *Wind Energy*;**22**:1848-71.

[7] Jin X, Xu Z, Qiao W. Condition monitoring of wind turbine generators using SCADA data Analysis 2021. *IEEE Transactions on Sustainable Energy*;**12**:202-10.

[8] Attallah O, Ibrahim RA, Zakzouk NE. Fault diagnosis for induction generator-based wind turbine using ensemble deep learning techniques 2022. *Energy Reports*;**8**:12787-98.

[9] Senemmar S, Zhang J. Deep Learning-based fault detection, classification, and locating in shipboard power systems 2021. In: *2021 IEEE Electric Ship Technologies Symposium (ESTS)*. Arlington, VA, USA: IEEE;. p. 1-6.

[10] Jacob RA, Senemmar S, Zhang J. Fault diagnostics in shipboard power systems using Graph Neural Networks 2021. In: *2021 IEEE 13th International Symposium on Diagnostics for Electrical Machines, Power Electronics and Drives (SDEMPED)*. vol. **1**;. p. 316-21.

[11] Senemmar S, Zhang J. Non-intrusive load monitoring in MVDC shipboard power systems using Wavelet-Convolutional Neural Networks 2022. In: *2022 IEEE Texas Power and Energy Conference (TPEC)*; 2022. p. 1-6.

[12] Senemmar S, Zhang J. Convolutional Wavelet Neural Network based non-intrusive load monitoring for next generation shipboard power systems 2023;.

[13] Mirzaeva G, Saad KI. Advanced diagnosis of stator turn-to-turn faults and static eccentricity in induction motors based on internal flux measurement 2018. *IEEE Transactions on Industry Applications*;**54**:3961-70.

[14] Wind Turbine - MATLAB & Simulink;. Available from: https://www.mathworks.com/help/sps/ug/wind-turbine.html.

[15] Dutta N, Kaliannan P, Shanmugam P. Application of machine learning for inter turn fault detection in pumping system. Scientific Reports. 2022 Jul;12(1):12906.

[16] Zsuga Dineva A. Data-driven onboard inter-turn short circuit fault diagnosis for electric vehicles by using real-time simulation environment. IEEE Access. 2023;11:145447-66.

[17] Nguyen V, Seshadrinath J, Wang D, Nadarajan S, Vaiyapuri V. Model-Based Diagnosis and RUL Estimation of Induction Machines Under Interturn Fault. IEEE Transactions on Industry Applications. 2017 May;53(3):2690-701.

[18] Nguyen VH. Model-based diagnosis and prognosis of induction motors under stator winding fault. Nanyang Technological University; 2018.

[19] Akansu AN, Haddad RA. In: 2001 *Multiresolution Signal Decomposition (2nd Edition)*. San Diego: Academic Press; 2001. p. 391-442.

[20] Malekian A, Chitsaz N. Concepts, procedures, and applications of artificial neural network models in streamflow forecasting 2021. In: *Advances in Streamflow Forecasting*. Elsevier;. p. 115-47.

[21] Hossin M, Sulaiman MN. A Review on Evaluation Metrics for Data Classification Evaluations. International Journal of Data Mining & Knowledge Management Process. 2015 Mar;5(2):01-11.